I&EC research
Industrial & Engineering Chemistry Research

Research Note

Cite This: Ind. Eng. Chem. Res. 2019, 58, 14603−14607

pubs.acs.org/IECR

Cerium Oxide Catalyzes the Selective Vapor-Phase Hydrodeoxygenation of Anisole to Benzene at Ambient Pressures of Hydrogen

Sadia Afrin and Praveen Bollini*

Department of Chemical & Biomolecular Engineering, University of Houston, 4726 Calhoun Rd., Houston, Texas 77004, United States

Supporting Information

ABSTRACT: Anisole hydrodeoxygenation data at 698 K and ambient pressures indicate that cerium oxide is a hydrogen-efficient catalyst that selectively cleaves carbon−oxygen bonds without hydrogenating aromatics. Phenol and benzene are the only major products observed, with benzene molar selectivity exceeding 85% at conversions greater than 7.7% (698 K, 102 kPa H_2, 0.07 kPa anisole, 0.008−0.042 $g_{anisole}\ g_{cat}^{-1}\ h^{-1}$). The catalyst exhibits less than 17% loss in conversion over the course of a 92-h run, and regeneration in air at 773 K returns conversion levels to that corresponding to the fresh catalyst. Benzene selectivity increases monotonically with hydrogen pressure at constant values of anisole conversion, demonstrating the potential for using hydrogen pressure (in addition to anisole conversion) as a lever to tune benzene selectivity. Overall, cerium oxide represents an inexpensive, highly selective, stable, regenerable, tunable, hydrogen-efficient catalyst that can hydrodeoxygenate biomass-derived model oxygenates at ambient pressures of hydrogen.

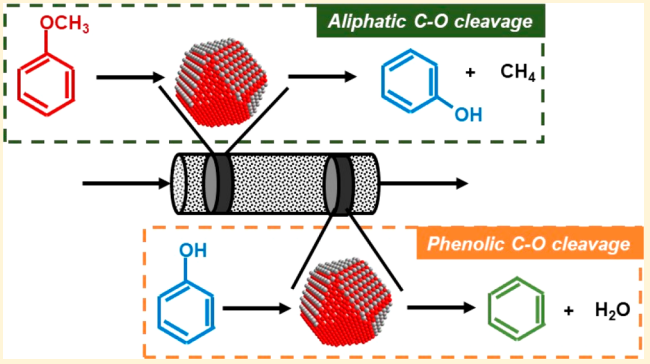

1. INTRODUCTION

Biomass conversion to fuels and chemicals represents a sustainable alternative to traditional fossil-based routes that currently account for approximately three-quarters of the world's energy supply.[1−6] Specifically, lignocellulosic biomass, which is more abundant than sugars and starchy crops,[7,8] less detrimental to the environment (from the standpoint of greenhouse gas emissions),[9,10] and noncompetitive with the food chain,[11] is an ideal source of renewable fuels and chemicals. Bio-oils derived from lignin deconstruction have several unfavorable characteristics—high acidities, viscosities, polarities, and corrosiveness, combined with low heating values and immiscibility with hydrocarbon fuels—that prevent their use as substitutes for fossil fuel-derived hydrocarbons.[12−14] The large-scale use of bio-oils as sources of fuels and chemicals is contingent on a reduction of their high oxygen content (10−40 wt %) which is, in large part, responsible for the aforementioned unfavorable characteristics.[1,15] Hydrodeoxygenation (HDO)—the removal of oxygen as water by cofeeding hydrogen—can be used to reduce the oxygen content of bio-oils, rendering them closer in value to conventional fossil fuel-derived hydrocarbons.[16]

Phenolic ethers are a major component of the products of lignin depolymerization,[17−19] and can be hydrodeoxygenated to form valuable chemicals such as benzene, toluene, and xylene. Anisole (methoxybenzene) is a widely used model compound in HDO studies, because of the presence of the methoxy group that is highly prevalent in lignin-derived phenolic ethers.[20−23] Achieving high selectivity to the desired product (benzene) is rendered challenging by several factors. First, achieving high selectivity to benzene requires either cleavage of the stronger phenolic C−O bond in anisole (homolytic bond dissociation energy (BDE) = 385 kJ mol^{-1}) over the weaker aliphatic C−O bond (BDE = 243 kJ mol^{-1}), or cleavage of an even stronger C−O bond in phenol formed in primary reactions (BDE = 460 kJ mol^{-1}) to form benzene in secondary reactions.[24] Second, high hydrogen pressures typically required to achieve C−O bond cleavage can result in a loss of aromaticity, resulting from HDO hydrogenation.[25−27] Third, side reactions such as C−C bond hydrogenolysis and alkylation/transalkylation can result in the formation of undesired side products.[28,29] These challenges have prompted researchers to not only look for new classes of catalysts but also to develop novel techniques including flame spray pyrolysis, for synthesizing traditional HDO catalysts,[30−33] and in situ spectroscopic techniques for developing mechanistic insights into HDO chemistry.[34−36] Despite the multitude of catalyst formulations that have been evaluated for the HDO of phenolic ethers, an inexpensive, easy to handle,

Received: April 11, 2019
Revised: July 15, 2019
Accepted: July 18, 2019
Published: July 18, 2019

DOI: 10.1021/acs.iecr.9b01987
Ind. Eng. Chem. Res. 2019, 58, 14603−14607

stable, highly selective HDO catalyst that operates at ambient pressures of hydrogen still remains elusive.

Cerium oxide, which is the most abundant rare-earth oxide in the Earth's crust,[37] is used commercially as an oxygen storage component in three-way catalysts for the treatment of automotive exhaust streams.[38,39] Apart from its abundance, low cost, and hydrothermal stability, cerium oxide is also endowed with the ability to act as a reversible sponge for oxygen—a property that enables its role as a buffer during lean-rich cycles that expose the catalyst to excess and substoichiometric amounts of oxygen, respectively.[40,41] Sievers and co-workers reported the HDO of guaiacol over ceria−zirconia materials at ambient pressures of hydrogen and 548−673 K.[42] The main strengths of the catalyst are 2-fold: the complete lack of hydrogenated products and no significant catalyst deactivation over the course of a 72-h long run. However, a relatively broad distribution of products, including anisole, catechol, benzene, cresol, and phenol, were observed in their experiments. Herein, we report the highly selective HDO of anisole to benzene over bulk ceria catalysts at ambient pressures of hydrogen. The catalyst shows no significant deactivation over the course of a 92-h run and a complete absence of hydrogenated products, exemplifying the principal features of an effective HDO catalyst.

2. EXPERIMENTAL SECTION

2.1. Catalyst Synthesis. Bulk cerium oxide was prepared using the procedure reported by Schimming et al.[42] Precipitation of cerium oxide was performed by adding cerium(III) nitrate hexahydrate (Acros Organics, 99.5%) to an aqueous solution of ammonium hydroxide (ACS reagent grade, 28%−30%). Specifically, a 0.1 M solution was prepared by dissolving 21.77 g of $Ce(NO_3)_3{\cdot}6H_2O$ in 498.6 g of deionized water. This solution was then added dropwise to 512 mL of aqueous NH_4OH with continuous stirring at a rate of 500 rpm over the course of 1.2 ks. The precipitate was filtered using a hand vacuum pump and rinsed twice with 50 mL of deionized water per 200 mL of solution filtered. The obtained powder was dried overnight at 373 K in an oven and calcined in a muffle furnace for 14.4 ks at 773 K under 3.33 $cm^3\ s^{-1}$ air (Matheson, zero-grade) with a ramp rate of 0.083 $K\ s^{-1}$, which is a procedure that is similar to other reports in the literature.[42,43] A quantity of 8.4 g of catalyst was recovered in the process and used for characterization and reactivity studies.

2.2. Material Characterization. Powder X-ray diffraction patterns were collected on a Rigaku SmartLab Diffractometer using Cu K-α radiation (40 kV, 30 mA) in the range 2θ = 20−80° with a step size of 0.02° and a scan rate of 0.167° s^{-1}. N_2 physisorption isotherms were measured using a Micromeritics 3 Flex instrument at 77 K, with the samples degassed at 473 K and 10.67−13.33 Pa for 14.4 ks.

2.3. Reactivity Studies. The catalyst sample was loaded in a quartz tube (inner diameter of 0.004 m) mounted in an insulated single-zone furnace (1060 W/115 V, Applied Test Systems Series 3210) with a thermocouple (Omega, Model KMQXL-062U-15) placed at the top of the catalyst bed, connected to an Applied Test Systems temperature controller (Model 17-16907), which was used to control the bed temperature and ramp rates. The sample was heated to 773 K at a ramp rate of 0.046 $K\ s^{-1}$ and then pretreated under a flow of 0.83 $cm^3\ s^{-1}$ air (Matheson, zero-grade) for 3.6 ks. Following pretreatment, the sample was cooled to reaction temperature (698 K) at 0.021 $K\ s^{-1}$ under air and purged with N_2 (0.83 $cm^3\ s^{-1}$, Matheson, ultrahigh-purity) for 3.6 ks. Vapor-phase anisole HDO reactions were performed by feeding a mixture containing anisole, H_2 (Matheson, ultrahigh-purity), ethane (internal standard) (2.01% in N_2, Praxair, certified standard), and N_2 (carrier) (Matheson, ultrahigh-purity). Anisole (Sigma, 99%, ReagentPlus) was fed using a syringe pump (KD Scientific, Model 100), with tubing downstream of the syringe pump heated to 373−393 K to prevent condensation of anisole and HDO products. Spent catalysts were regenerated at 773 K under 0.83 $cm^3\ s^{-1}$ air for 28.8 ks. Product molar flow rates were quantified using a flame ionization detector on an Agilent Model 7890B gas chromatograph that was equipped with a methyl-siloxane capillary column (HP-1, 30 m × 320 μm × 3 μm). Anisole conversion was calculated by comparing the total molar flow rate of aromatics by the inlet flow rate of anisole.

3. RESULTS AND DISCUSSION

3.1. Selectivity. One of the key challenges in achieving high selectivity to benzene in the hydrodeoxygenation of anisole is the mitigation of hydrogenation reactions that result in a loss of aromaticity. Such inefficient use of hydrogen is reflected in non-negligible selectivity to hydrogenated products reported during anisole HDO over traditional hydrotreating catalysts such as cobalt−molybdenum sulfide on alumina,[44,45] copper chromite,[46] supported noble metal,[47,48] transition-metal phosphide,[49] and carbide catalysts.[21] Anisole HDO over cerium oxide at 698 K yields exclusively aromatic products with no traces of hydrogenated compounds detected in the product stream, thus exhibiting complete hydrogen efficiency, where hydrogen efficiency is defined as the fraction of hydrogen consumed in the reactor exclusively to break carbon−oxygen bonds. The only C_6^+ products observed are phenol, benzene, toluene, cresol, and an unidentified C_{12}^+ oligomer, with no C_2−C_5 products resulting from C−C bond hydrogenolysis detected. Methane was the only aliphatic product observed under these conditions, with methanol being absent from the product stream at all conversions tested in this study, suggesting that hydrodeoxygenation to benzene proceeded through cleavage of the aliphatic C−O bond to form phenol and methane in primary reactions, and phenol undergoing hydrodeoxygenation to form benzene in secondary reactions. The absence of methanol production is similar in nature to anisole HDO data reported on cobalt−molybdenum sulfide and noble-metal catalysts,[45,50,51] but is in contrast with the performance of molybdenum carbide catalysts that show increasing methane and decreasing methanol selectivities with anisole conversion.[21,52] Confirmation of the rank of these two steps and mechanisms mediating their turnovers will require a more-detailed kinetic study, which is not the focus of this Research Note. Rather, we emphasize here the fact that ceria catalyst under investigation exhibits >85% molar selectivity to benzene at conversions of >7.7% at 698 K, with phenol, toluene, and cresol being minor products (Figure 1). Such high selectivity to benzene during anisole HDO is in contrast with most of the aforementioned classes of catalysts, for which benzene comprises less than half the product carbon.[22,45,46,50,51,53] We note that the lack of hydrogenated products observed in this study has similarities to the HDO data over molybdenum oxide reported by Román-Leshkov and co-workers.[54,55] As discussed above, selective formation of benzene is contingent on either cleaving the stronger phenolic

DOI: 10.1021/acs.iecr.9b01987
Ind. Eng. Chem. Res. 2019, 58, 14603−14607

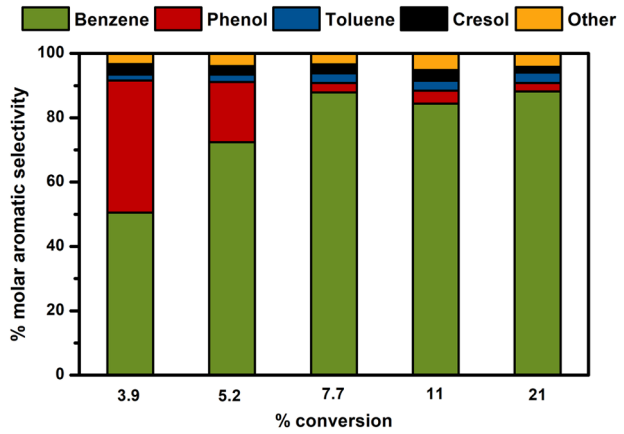

Figure 1. Product distribution, as a function of anisole conversion. [Conditions: 698 K, 102 kPa H_2, 0.07 kPa anisole, 0.008−0.042 $g_{anisole}$ g_{cat}^{-1} h^{-1}.]

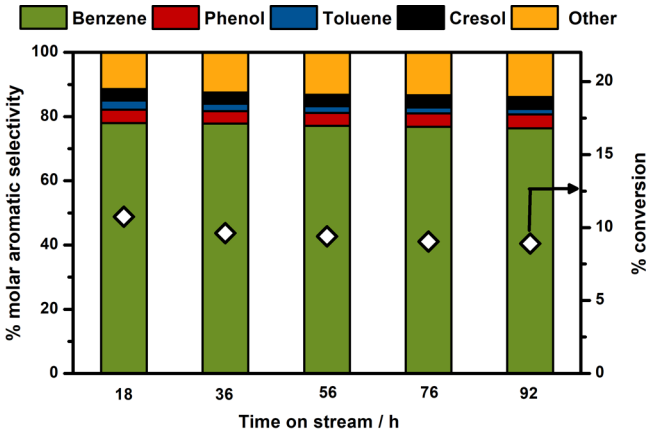

Figure 2. Time-on-stream dependence of conversion and product distribution in the hydrodeoxygenation (HDO) of anisole. [Conditions: 698 K, 105 kPa H_2, 0.07 kPa anisole, 0.24 g CeO_2, 0.042 $g_{anisole}$ g_{cat}^{-1} h^{-1}.]

C−O bond in anisole or cleaving the even-stronger phenolic C−O bond in phenol formed in primary steps of anisole HDO, both of which have proven to be highly challenging. This unfavorable order of homolytic BDEs constitutes at least part of the explanation as to why phenol is typically reported to be the major product in anisole HDO over traditional hydrotreating catalysts.[45,50,53]

3.2. Catalyst Lifetime and Regenerability. One of the major challenges in designing effective HDO catalysts is overcoming catalyst deactivation, which has been shown to adversely affect HDO performance of several classes of catalysts evaluated in the literature. For example, silica-supported phosphorus-modified sulfided Co−Mo−W catalysts showed a 19%−72% loss in HDO activity within the first 4 h at 3 MPa and 583 K.[53] Zhu et al. reported a 60% decrease in anisole conversion over 1 wt % platinum supported on silica or HBEA zeolite at 673 K and atmospheric pressure.[23] Li et al. reported a 30% decrease in anisole conversion over 0.5 wt % Ni−Mo phosphide supported on silica at 573 K and 1.5 MPa over the course of a 10-h run, with a concurrent increase in benzene selectivity at the expense of cyclohexane selectivity.[22] Interestingly, MoO_3 (a reducible oxide), although highly hydrogen-efficient, also shows a 40% drop in anisole conversion in the first couple of hours at 673 K and atmospheric pressure.[56] The cerium oxide catalyst reported in this study shows minimal changes in both conversion and product distribution during anisole HDO at 698 K over the course of a 92-h run (Figure 2). Conversion decreases by 10% between 18 h and 36 h on stream with a negligible rate of change in conversion after the first 36 h, demonstrating that cerium oxide, in addition to being highly selective to benzene, is also resistant to deactivation. Moreover, minor changes in conversion and product distribution were recovered upon regenerating under air at 773 K for 28.8 ks (Figure 3), demonstrating regenerability of the catalyst. The lower bound for the turnover number, calculated by assuming every surface oxygen atom to be an active site for this chemistry over a 92-h run, was calculated to be 2, demonstrating that the process is catalytic in nature (detailed calculations are presented in section S3 in the Supporting Information). The precise cause of the rather-limited amount of catalyst deactivation is not well-understood at this point, but a decrease in pore volume and surface area of the spent catalyst compared to the fresh catalyst that can partly be recovered upon regeneration in air at

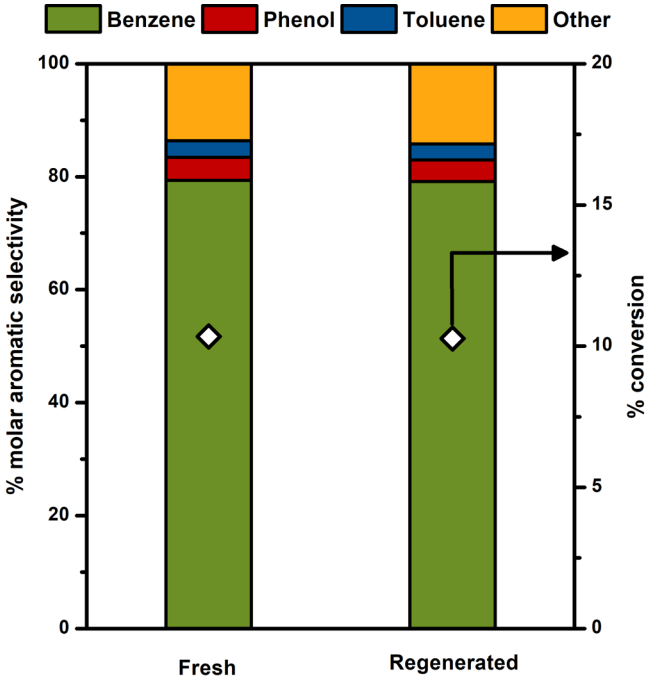

Figure 3. Conversion and product distribution for fresh and regenerated ceria. [Conditions: 698 K, 109 kPa H_2, 0.07 kPa anisole, 0.042 $g_{anisole}$ g_{cat}^{-1} h^{-1}; regeneration: 0.83 cm^3 s^{-1} air, 773 K, 28.8 ks.]

773 K (see Figure S4 in the Supporting Information) suggests that carbon deposition blocking active sites may contribute to at least part of the decrease in conversion.

3.3. Tunable Benzene Selectivity. As shown above, benzene molar selectivities in excess of 85% can be achieved at 102 kPa of H_2 and 698 K. We note an additional interesting kinetic phenomenon that results in a monotonic increase in benzene selectivity as a function of hydrogen pressure at isoconversion (8.4−10.7% anisole conversion, Figure 4). Comparison at isoconversion is necessitated by the fact that increasing the hydrogen pressure at a constant space velocity and anisole pressure leads to an increase in conversion, which, in and of itself can result in an increase in benzene selectivity, as shown in section 3.1. The mechanistic basis for such an increase in benzene selectivity and the concurrent decrease in

DOI: 10.1021/acs.iecr.9b01987
Ind. Eng. Chem. Res. 2019, 58, 14603−14607

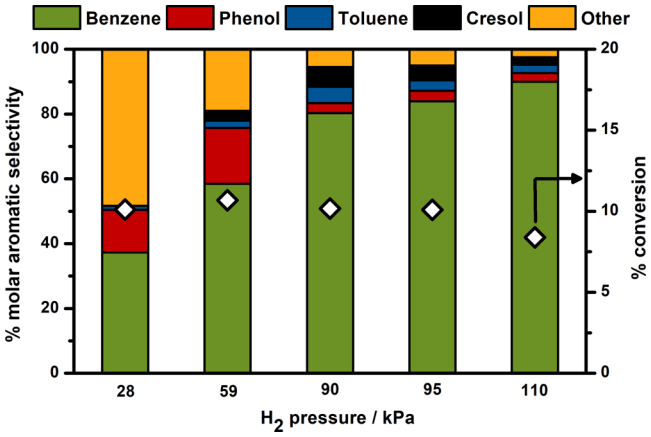

Figure 4. Product distribution as a function of hydrogen pressure at constant anisole conversion. [Conditions: 698 K, 0.07 kPa anisole, 0.008−0.028 $g_{anisole}$ g_{cat}^{-1} h^{-1}.]

phenol selectivity is not understood at this point, but does demonstrate that benzene selectivity can be tuned systematically merely by varying the hydrogen pressure.

4. CONCLUSIONS

Cerium oxide is a low-cost, abundant, stable, highly selective, tunable, hydrogen-efficient hydrodeoxygenation (HDO) catalyst that exhibits >85% selectivity to benzene in the HDO of anisole at ambient pressures of hydrogen. Minor changes (≤17%) in anisole conversion and product distribution observed over the course of a 92-h run can be recovered on regeneration in air at 773 K. The selectivity to the desired product, benzene, can be tuned at isoconversion merely by varying hydrogen pressure. The mechanistic basis for this behavior, in addition to the highly favorable performance of cerium oxide in anisole HDO, is not well understood at this point and is currently under investigation in our research group.

■ ASSOCIATED CONTENT

Supporting Information

The Supporting Information is available free of charge on the ACS Publications website at DOI: 10.1021/acs.iecr.9b01987.

Powder X-ray diffraction patterns of catalyst samples (Figure S1); N_2 physisorption isotherms of catalyst samples (Figure S2); calculation of turnover number for anisole HDO over bulk cerium oxide (Figure S3); compilation of literature data on hydrodeoxygenation of aromatic oxygenates (Figure S4); and C1 (methane) to C6 (benzene + phenol) molar ratio as a function of H_2 pressure (Figure S5) (PDF)

■ AUTHOR INFORMATION

Corresponding Author

*E-mail: ppbollini@uh.edu.

ORCID

Praveen Bollini: 0000-0001-8092-8092

Notes

The authors declare no competing financial interest.

■ REFERENCES

(1) Huber, G. W.; Iborra, S.; Corma, A. Synthesis of Transportation Fuels from Biomass. *Chem. Rev.* **2006**, *106*, 4044−4098.
(2) Chheda, J. N.; Huber, G. W.; Dumesic, J. A. Liquid-Phase Catalytic Processing of Biomass-Derived Oxygenated Hydrocarbons to Fuels and Chemicals. *Angew. Chem., Int. Ed.* **2007**, *46*, 7164−7183.
(3) Bridgwater, A. V. Catalysis in Thermal Biomass Conversion. *Appl. Catal., A* **1994**, *116*, 5−47.
(4) Demirbaş, A. Biomass Resource Facilities and Biomass Conversion Processing for Fuels and Chemicals. *Energy Convers. Manage.* **2001**, *42*, 1357−1378.
(5) Lin, Y.-C.; Huber, G. W. The Critical Role of Heterogeneous Catalysis in Lignocellulosic Biomass Conversion. *Energy Environ. Sci.* **2009**, *2*, 68−80.
(6) Gallezot, P. Catalytic Conversion of Biomass: Challenges and Issues. *ChemSusChem* **2008**, *1*, 734−737.
(7) Limayem, A.; Ricke, S. C. Lignocellulosic Biomass for Bioethanol Production: Current Perspectives, Potential Issues and Future Prospects. *Prog. Energy Combust. Sci.* **2012**, *38*, 449−467.
(8) Taha, M.; Foda, M.; Shahsavari, E.; Aburto-Medina, A.; Adetutu, E.; Ball, A. Commercial Feasibility of Lignocellulose Biodegradation: Possibilities and Challenges. *Curr. Opin. Biotechnol.* **2016**, *38*, 190−197.
(9) Zabed, H.; Sahu, J. N.; Boyce, A. N.; Faruq, G. Fuel Ethanol Production from Lignocellulosic Biomass: An Overview on Feedstocks and Technological Approaches. *Renewable Sustainable Energy Rev.* **2016**, *66*, 751−774.
(10) Hahn-Hägerdal, B.; Galbe, M.; Gorwa-Grauslund, M. F.; Lidén, G.; Zacchi, G. Bio-Ethanol - the Fuel of Tomorrow from the Residues of Today. *Trends Biotechnol.* **2006**, *24*, 549−556.
(11) Zhao, J.; Xia, L. Ethanol Production from Corn Stover Hemicellulosic Hydrolysate Using Immobilized Recombinant Yeast Cells. *Biochem. Eng. J.* **2010**, *49*, 28−32.
(12) Bridgwater, A. V.; Peacocke, G. V. C. Fast Pyrolysis Processes for Biomass. *Renewable Sustainable Energy Rev.* **2000**, *4*, 1−73.
(13) Carlson, T. R.; Tompsett, G. A.; Conner, W. C.; Huber, G. W. Aromatic Production from Catalytic Fast Pyrolysis of Biomass-Derived Feedstocks. *Top. Catal.* **2009**, *52*, 241−252.
(14) Venderbosch, R. H.; Prins, W. Fast Pyrolysis Technology Development. *Biofuels, Bioprod. Biorefin.* **2010**, *4*, 178−208.
(15) Bui, V. N.; Laurenti, D.; Delichère, P.; Geantet, C. Hydrodeoxygenation of Guaiacol. Part II: Support Effect for CoMoS Catalysts on HDO Activity and Selectivity. *Appl. Catal., B* **2011**, *101*, 246−255.
(16) Furimsky, E. Catalytic Hydrodeoxygenation. *Appl. Catal., A* **2000**, *199*, 147−190.
(17) Thring, R. W.; Breau, J. Hydrocracking of Solvolysis Lignin in a Batch Reactor. *Fuel* **1996**, *75*, 795−800.
(18) Britt, P. F.; Buchanan, A. C.; Cooney, M. J.; Martineau, D. R. Flash Vacuum Pyrolysis of Methoxy-Substituted Lignin Model Compounds. *J. Org. Chem.* **2000**, *65*, 1376−1389.
(19) Yan, N.; Yuan, Y.; Dykeman, R.; Kou, Y.; Dyson, P. J. Hydrodeoxygenation of Lignin-Derived Phenols into Alkanes by Using Nanoparticle Catalysts Combined with Brønsted Acidic Ionic Liquids. *Angew. Chem., Int. Ed.* **2010**, *49*, 5549−5553.
(20) Li, C.; Xing, J.; Li, W.; Jin, S.; Xiao, Z.; Wang, L.; Chen, X.; Liang, C. Catalytic Hydrodeoxygenation of Anisole as Lignin Model Compound over Supported Nickel Catalysts. *Catal. Today* **2014**, *234*, 125−132.
(21) Lee, W. S.; Kumar, A.; Wang, Z.; Bhan, A. Chemical Titration and Transient Kinetic Studies of Site Requirements in Mo2C-Catalyzed Vapor Phase Anisole Hydrodeoxygenation. *ACS Catal.* **2015**, *5*, 4104−4114.
(22) Li, K.; Wang, R.; Chen, J. Hydrodeoxygenation of Anisole over Silica-Supported Ni_2P, MoP, and NiMoP Catalysts. *Energy Fuels* **2011**, *25*, 854−863.
(23) Zhu, X.; Lobban, L. L.; Mallinson, R. G.; Resasco, D. E. Bifunctional Transalkylation and Hydrodeoxygenation of Anisole over a Pt/HBeta Catalyst. *J. Catal.* **2011**, *281*, 21−29.

DOI: 10.1021/acs.iecr.9b01987
Ind. Eng. Chem. Res. 2019, 58, 14603−14607

(24) Prasomsri, T.; Shetty, M.; Murugappan, K.; Roman-Leshkov, Y. Insights into the Catalytic Activity and Surface Modi Fi Cation of MoO_3 during the Hydrodeoxygenation of Lignin-Derived Model. *Energy Environ. Sci.* **2014**, *7*, 2660−2669.
(25) Ohta, H.; Kobayashi, H.; Hara, K.; Fukuoka, A. Hydrodeoxygenation of Phenols as Lignin Models under Acid-Free Conditions with Carbon-Supported Platinum Catalysts. *Chem. Commun.* **2011**, *47*, 12209−12211.
(26) Zhao, C.; Kou, Y.; Lemonidou, A. A.; Li, X.; Lercher, J. A. Highly Selective Catalytic Conversion of Phenolic Bio-Oil to Alkanes. *Angew. Chem., Int. Ed.* **2009**, *48*, 3987−3990.
(27) He, J.; Zhao, C.; Lercher, J. A. Ni-Catalyzed Cleavage of Aryl Ethers in the Aqueous Phase. *J. Am. Chem. Soc.* **2012**, *134*, 20768−20775.
(28) Anderson, E.; Crisci, A.; Murugappan, K.; Roman-Leshkov, Y. Bifunctional Molybdenum Polyoxometalates for the Combined Hydrodeoxygenation and Alkylation of Lignin- Derived Model Phenolics. *ChemSusChem* **2017**, *10*, 2226−2234.
(29) Saidi, M.; Rostami, P.; Rahimpour, H. R.; Roshanfekr Fallah, M. A.; Rahimpour, M. R.; Gates, B. C.; Raeissi, S. Kinetics of Upgrading of Anisole with Hydrogen Catalyzed by Platinum Supported on Alumina. *Energy Fuels* **2015**, *29*, 4990−4997.
(30) Kim, K. D.; Pokhrel, S.; Wang, Z.; Ling, H.; Zhou, C.; Liu, Z.; Hunger, M.; Mädler, L.; Huang, J. Tailoring High-Performance Pd Catalysts for Chemoselective Hydrogenation Reactions via Optimizing the Parameters of the Double-Flame Spray Pyrolysis. *ACS Catal.* **2016**, *6*, 2372−2381.
(31) Schimmoeller, B.; Hoxha, F.; Mallat, T.; Krumeich, F.; Pratsinis, S. E.; Baiker, A. Fine Tuning the Surface Acid/Base Properties of Single Step Flame-Made Pt/Alumina. *Appl. Catal., A* **2010**, *374*, 48−57.
(32) Huang, J.; Jiang, Y.; Van Vegten, N.; Hunger, M.; Baiker, A. Tuning the Support Acidity of Flame-Made Pd/SiO_2-Al_2O_3 Catalysts for Chemoselective Hydrogenation. *J. Catal.* **2011**, *281*, 352−360.
(33) Strobel, R.; Stark, W. J.; Mädler, L.; Pratsinis, S. E.; Baiker, A. Flame-Made Platinum/Alumina: Structural Properties and Catalytic Behaviour in Enantioselective Hydrogenation. *J. Catal.* **2003**, *213*, 296−304.
(34) Chen, M.; Maeda, N.; Baiker, A.; Huang, J. Hydrogenation of Acetophenone on Pd/Silica-Alumina Catalysts with Tunable Acidity: Mechanistic Insight by in Situ ATR-IR Spectroscopy. *ACS Catal.* **2018**, *8*, 6594−6600.
(35) Iino, A.; Takagaki, A.; Kikuchi, R.; Oyama, S. T.; Bando, K. K. Combined in Situ XAFS and FTIR Study of the Hydrodeoxygenation Reaction of 2-Methyltetrahydrofuran on Ni_2P/SiO_2. *J. Phys. Chem. C* **2019**, *123*, 7633−7643.
(36) Moon, J. S.; Lee, Y. K. Support Effects of Ni_2P Catalysts on the Hydrodeoxygenation of Guaiacol: In Situ XAFS Studies. *Top. Catal.* **2015**, *58*, 211−218.
(37) Reinhardt, K.; Winkler, H. Cerium Mischmetal, Cerium Alloys, and Cerium Compounds. *Ullmann's Encyclopedia of Industrial Chemistry* **2000**, *8*, 531−621.
(38) Shelef, M.; Graham, G. W.; McCabe, R. W. *Ceria and Other Oxygen Storage Components in Automotive Catalysts*; Trovarelli, A., Ed.; Catalytic Science Series, Vol. *2*; World Scientific: Singapore, 2002; pp 343−375 (DOI: 10.1142/9781860949654_0010).
(39) Trovarelli, A. Catalytic Properties of Ceria. *Catal. Rev.: Sci. Eng.* **1996**, *38*, 439−520.
(40) Yao, H. C.; Yao, Y. F. Y. Ceria in Automotive Exhaust Catalysts. I. Oxygen Storage. *J. Catal.* **1984**, *86*, 254−265.
(41) Ji, Y.; Toops, T. J.; Crocker, M. Effect of Ceria on the Storage and Regeneration Behavior of a Model Lean NO_x Trap Catalyst. *Catal. Lett.* **2007**, *119*, 257−264.
(42) Schimming, S. M.; Lamont, O. D.; König, M.; Rogers, A. K.; D'Amico, A. D.; Yung, M. M.; Sievers, C. Hydrodeoxygenation of Guaiacol over Ceria-Zirconia Catalysts. *ChemSusChem* **2015**, *8*, 2073−2083.
(43) Rossignol, S.; Madier, Y.; Duprez, D. Preparation of Zirconia-Ceria Materials by Soft Chemistry. *Catal. Today* **1999**, *50*, 261−270.
(44) Viljava, T.-R.; Komulainen, R. S.; Krause, A. O. I. Effect of H_2S on the Stability of $CoMo/A_2O_3$ Catalysts during Hydrodeoxygenation. *Catal. Today* **2000**, *60*, 83−92.
(45) Hurff, S. J.; Klein, M. T. Reaction Pathway Analysis of Thermal and Catalytic Lignin Fragmentation by Use of Model Compounds. *Ind. Eng. Chem. Fundam.* **1983**, *22*, 426−430.
(46) Deutsch, K. L.; Shanks, B. H. Hydrodeoxygenation of Lignin Model Compounds over a Copper Chromite Catalyst. *Appl. Catal., A* **2012**, *447*−*448*, 144−150.
(47) Phan, T. N.; Park, Y.; Lee, I.; Ko, C. H. Enhancement of C-O Bond Cleavage to Afford Aromatics in the Hydrodeoxygenation of Anisole over Ruthenium-Supporting Mesoporous Metal Oxides. *Appl. Catal., A* **2017**, *544*, 84−93.
(48) Gamliel, D. P.; Karakalos, S.; Valla, J. A. Liquid Phase Hydrodeoxygenation of Anisole, 4-Ethylphenol and Benzofuran Using Ni, Ru and Pd Supported on USY Zeolite. *Appl. Catal., A* **2018**, *559*, 20−29.
(49) Li, Y.; Fu, J.; Chen, B. Highly Selective Hydrodeoxygenation of Anisole, Phenol and Guaiacol to Benzene over Nickel Phosphide. *RSC Adv.* **2017**, *7*, 15272−15277.
(50) Jongerius, A. L.; Jastrzebski, R.; Bruijnincx, P. C. A.; Weckhuysen, B. M. CoMo Sulfide-Catalyzed Hydrodeoxygenation of Lignin Model Compounds : An Extended Reaction Network for the Conversion of Monomeric and Dimeric Substrates. *J. Catal.* **2012**, *285*, 315−323.
(51) Runnebaum, R. C.; Nimmanwudipong, T.; Block, D. E.; Gates, B. C. Catalytic Conversion of Anisole : Evidence of Oxygen Removal in Reactions with Hydrogen. *Catal. Lett.* **2011**, *141*, 817−820.
(52) Lee, W. S.; Wang, Z.; Wu, R. J.; Bhan, A. Selective Vapor-Phase Hydrodeoxygenation of Anisole to Benzene on Molybdenum Carbide Catalysts. *J. Catal.* **2014**, *319*, 44−53.
(53) Loricera, C. V.; Pawelec, B.; Infantes-Molina, A.; Álvarez-Galván, M. C.; Huirache-Acuña, R.; Nava, R.; Fierro, J. L. G. Hydrogenolysis of Anisole over Mesoporous Sulfided CoMoW/SBA-15(16) Catalysts. *Catal. Today* **2011**, *172*, 103−110.
(54) Shetty, M.; Murugappan, K.; Prasomsri, T.; Green, W. H.; Román-Leshkov, Y. Reactivity and Stability Investigation of Supported Molybdenum Oxide Catalysts for the Hydrodeoxygenation (HDO) of m-Cresol. *J. Catal.* **2015**, *331*, 86−97.
(55) Prasomsri, T.; Shetty, M.; Murugappan, K.; Román-Leshkov, Y. Insights into the Catalytic Activity and Surface Modification of MoO_3 during the Hydrodeoxygenation of Lignin-Derived Model Compounds into Aromatic Hydrocarbons under Low Hydrogen Pressures. *Energy Environ. Sci.* **2014**, *7*, 2660−2669.
(56) Prasomsri, T.; Nimmanwudipong, T.; Román-Leshkov, Y. Effective Hydrodeoxygenation of Biomass-Derived Oxygenates into Unsaturated Hydrocarbons by MoO_3 Using Low H_2 Pressures. *Energy Environ. Sci.* **2013**, *6*, 1732−1738.

DOI: 10.1021/acs.iecr.9b01987
Ind. Eng. Chem. Res. 2019, 58, 14603−14607